Gait & Posture 46 (2016) 179–183

Contents lists available at ScienceDirect

Gait & Posture

journal homepage: www.elsevier.com/locate/gaitpost

Evaluation of a force plate system for measuring center of pressure in railroad ballast

Hang Xu [a,b], Andrew Merryweather [b,*], Donald Bloswick [b]

[a] School of Medical Imaging, Xuzhou Medical College, Xuzhou, PR China
[b] Department of Mechanical Engineering, University of Utah, Salt Lake City, UT, USA

ARTICLE INFO

Article history:
Received 13 October 2015
Received in revised form 10 February 2016
Accepted 14 March 2016

Keywords:
Force plate
Center of pressure
Railroad ballast
Instrumentation validity

ABSTRACT

Traditional biomechanical analyses have focused primarily on the human gait across hard, flat surfaces and provide little information about human locomotion as a function of work environment or terrain. The purpose of this study was evaluation of a force plate system for measure of center of pressure (COP) in railroad ballast by comparing its accuracy across three surface conditions (hard surface, mainline ballast and walking ballast) with two configurations (level and 7° cross-slope). Custom walkways and an isolation fixture were developed to rigidly attach a force plate beneath ballast surfaces to collect the COP. The difference in COP location ($\Delta COPx$, y, z) between the force plate system and a calibration system (motion capture derived) were compared using repeated-measures analysis of variance. Results indicate that the effects of surface condition and configuration were not significant for $\Delta COPx$, y, z and no differences were found among the three surface conditions during pairwise comparison, though $\Delta COPx$, y, z were different between the center and corners of the force plate in ballasts for both level and cross-slope configurations. The system presented in this study demonstrates the feasibility of measuring the COP by using an isolation-fixture force plate to expand the scope of biomechanical studies on ballast surfaces that are level or cross-slope.

1. Introduction

The biomechanics of human gait have been studied extensively in the past decade with most gait analysis conducted on level, hard surfaces including indoor tracks and treadmills [1–4]. However, work environments may include a variety of terrain and walking conditions. Recently, research has extended our understanding of human locomotion on other surface conditions, like sand, grass and rock [5–11], and configurations, like inclines/declines [12–14] and cross-slope [15–17]. A few studies investigated the energy costs and kinematics when walking on sand or grass, but not kinetics due to the challenges of validating the accuracy and reliability of force plate measurement on these altered conditions [5–7]. Other research investigated lower limb biomechanics when walking on sloped surfaces at various gradients; validation of tilted force plate systems has also been performed [13,15,16]. These studies indicated that significant differences exist in ground reaction force, kinematics and kinetics while walking on sloped conditions compared to level conditions, and further our understanding of gait adaptation on non-level surfaces.

Several studies looked into the gait characteristics during locomotion on ballast (crush rock aggregate) and a cross-slope condition [10,11,18], which is the occupational environment for many workers employed in the rail industry. The two primary ballast types were defined as walking ballast (WB, diameter 9.53–31.75 mm), generally located in railroad yards, and mainline ballast (MB, diameter 19.05–63.5 mm), generally located on main track lines. Andres et al. [10] reported that walking on cross-slope MB significantly increased the rear foot range of motion compared to walking on either WB or no ballast (NB). Merryweather et al. [18] found that a significant increase in knee flexion and foot clearance was required to prevent trip potentials while walking on ballast compared to hard surfaces in level and cross-slope situations. Wade and Redfern [19] investigated a method to measure ground reaction force using a force plate embedded beneath 63.5-mm and 101.6-mm of ballast. This method suggested that measuring reaction force with ballast applied to the top surface of the force plate was

* Corresponding author at: Department of Mechanical Engineering, University of Utah, 1495 E. 100 S., Salt Lake City, UT 84112, USA. Tel.: +1 801 581 8118; fax: +1 801 585 5261.
E-mail address: a.merryweather@utah.edu (A. Merryweather).

http://dx.doi.org/10.1016/j.gaitpost.2016.03.013
0966-6362/

feasible in level conditions. However, the approach might be inappropriate for measurements with greater ballast depths, where the effects of force dissipation would most likely increase, especially along the edge of the force plate. It is unclear whether or not their setup would be appropriate for cross-slope conditions. A following study conducted by Wade et al. [11] utilized this force plate system to study gait biomechanics on ballast and reported that joint moment ranges were smaller, but the muscle co-contraction levels were greater on ballast compared with NB in level condition.

The purpose of this study was to evaluate a custom, slope-adjustable walkway system with an isolation fixture for the force plate to determine the center of pressure (COP). In order to validate this walkway system, a calibration system, including a rigid mechanical device and associated software, was utilized to determine the COP. This walkway system is proposed to expand the capabilities to study biomechanics, including gait for various activities on railroad ballast.

2. Methods

Two custom walkways were designed and constructed of engineering I-beams to provide the ability to test multiple experimental conditions including varying walking surfaces and cross-slopes. It was of particular interest to study two types of ballast (WB and MB) and two configurations (level and cross-slope of 7°) to resemble the typical environments encountered by railroad employees working in the railyard or on the mainline [10]. Each walkway was 23 cm deep and provided a working surface 76-cm wide by 7.3-m long with an embedded force plate (model OR6-5-1000, AMTI, Watertown, MA) to record reaction force and the COP. Ten adjustable jacks were placed on each walkway so one side of the walkway could be elevated to generate the cross-slope condition (Fig. 1a–c). WB and MB were filled 20-cm depth in two walkways similar to the previous study, and then compacted by ballast tamper (similar to Model MRC 1100 P, FCS Rail Inc., Italy) to produce consolidation and reduce shifting to resemble ballast in normal railroad conditions other than freshly laid or disturbed ballast [10,20].

A custom isolation fixture was developed to isolate surrounding ballast from ballast directly in contact with the force plate. The isolation fixture consisted of two welded, concentrically aligned steel rectangle frames with 6.4-mm clearance between the inner and outer frame walls. The fixture was open from the top to bottom and ballast can be applied to the top surface of the force plate (Fig. 1d–f). The outer frame was securely attached to the base of each walkway and the inner frame securely fit on the force plate with four alignment tabs. The tabs served to "lock" the inner frame to the force plate to translate shear forces to the force plate from ballast.

Five digital video camcorders (PV-GS55, Panasonic Corporation of North America, Secaucus, NJ) were configured around the walkway setup to allow for a motion capture volume of 6.8 m^3. The laboratory coordinate system was oriented with z-axis upward, x-axis anterior/posterior, and y-axis medial/lateral. The force plate coordinate system was oriented with the z-axis directed downwards toward the surface of the force plate; these two coordinate systems were related using a transformation/rotation matrix.

The COPs derived from the force plate in the NB condition were calculated using Eqs. (1) and (2), where x and y were the coordinates of COP in the horizontal plane. Fs and Ms were the components of force and moment vectors as determined from the force plate. The values a, b, c are the configuration data of the true origin of the force plate which were determined by the manufacturer as part of the calibration procedure and supplied with the force platform. When ballast was placed on the force plate in the isolation fixture, the force plate origin relative to the contact surface plane was adjusted; therefore, the COPs were calculated using Eqs. (3) and (4), where t was the average ballast depth above the top surface of the force plate, which was 0.2 m in this study.

$$x = -\frac{M_y + cF_x}{F_z} + a \tag{1}$$

$$y = \frac{M_x - cF_y}{F_z} + b \tag{2}$$

$$x = -\frac{M_y + (c-t)F_x}{F_z} + a \tag{3}$$

$$y = \frac{M_x - (c-t)F_y}{F_z} + b \tag{4}$$

The calibration system included a rigid mechanical testing device (MTD) (Motion Lab Systems, Baton Rouge, LA) and associated software (CalTester, C-Motion Inc., Germantown, MD) that was used to validate the ability to accurately measure the COP in this custom, slope-adjustable walkway system. The MTD was designed with five reflective markers on wands attached to a calibration-testing rod with two conical tips, a test plate and a handle (Fig. 2a). The conical tips provided a way for direct force to be applied with a negligible applied moment or force couple [21,22]. The test plate was designed to rest on the surface of the force plate and had a machined conical impression in the center to constrain the conical tip and allow force to be applied near the corners of the force plate. The handle was a rigid bar with a machined conical impression for applying force to the MTD. The tip of the MTD rod location was determined by the motion capture component combined with the relative location information of reflective markers. For each trial, the test plate was placed at one of five locations on the force plate, including the four corners and the center.

A member of the research team placed the MTD on the base plate and applied a force (135 ± 27 N) through the rod by pressing down on the handle. While applying the force, the researcher pivoted the rod through a circular pattern along the vertical axis of the laboratory coordinate system according to the instructions provided by CalTester [21]. This procedure was followed at each location on the force plate for each surface condition and configuration.

Five trials were conducted at the four corners and the center of the force plate for each of six test conditions (NB level, NB cross-slope, MB level, MB cross-slope, WB level and WB cross-slope) for a total of 150 trials. Before conducting a trial, a known weight (44.5 N) was placed on the center and each of the corners for each condition/configuration to verify the force readings perpendicular to the plate surface, which was 44.022 ± 0.396 N and 43.932 ± 0.254 N in level and cross-slope conditions on average, respectively. Then, dynamic trials were performed with the MTD. Each dynamic trial consisted of a 15-s time period at each location. A member of the research team controlled the angle of the MTD while applying force. The video data and analog data were recorded simultaneously. Motion data were collected at 60 Hz using a motion capture system (Vicon Motion Systems, Centennial, CO) and then conditioned using a fourth order zero-lag Butterworth filter with a cutoff frequency of 6 Hz. Force plate data were recorded at 600 Hz. Data points where the applied vertical force was less than 20 N were excluded for analysis due to the sensitivity of calculated COP to small vertical forces (Eqs. (1) and (2)) [23,24].

For each trial, the data calculated using CalTester software provided the coincidence information between these two systems

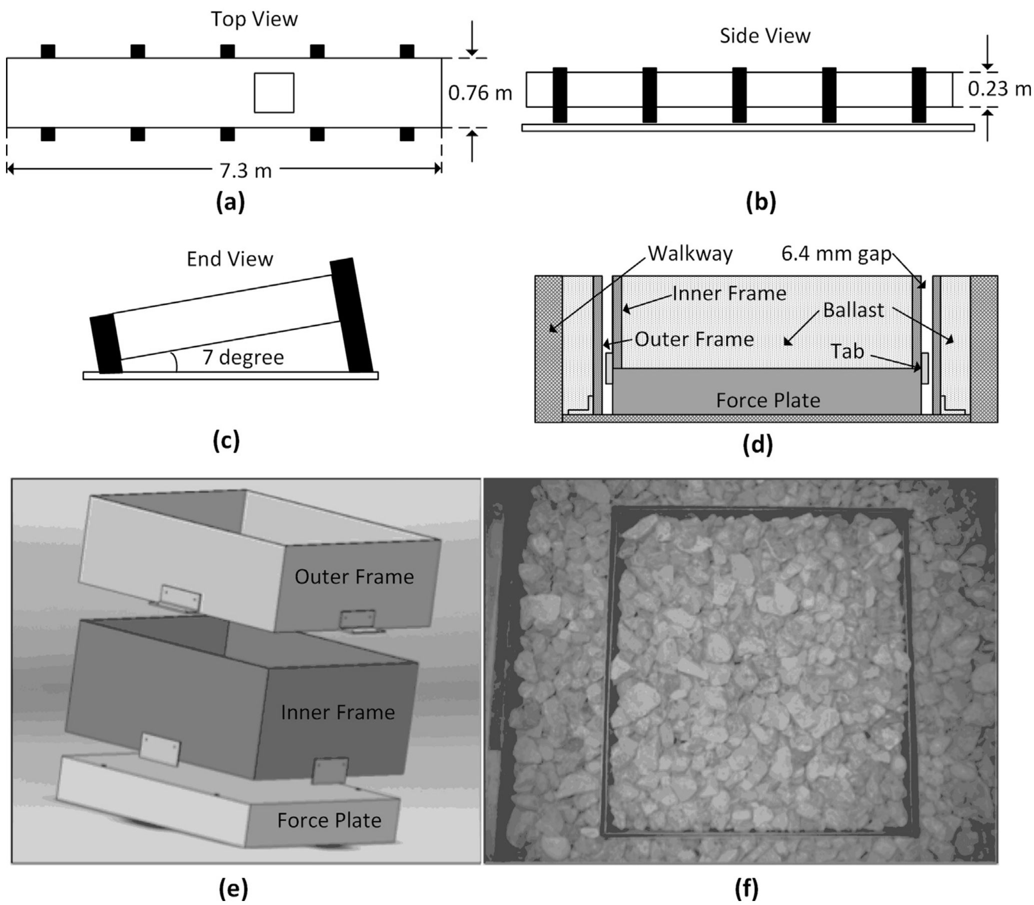

Fig. 1. The custom build walkway to simulate railyard conditions: (a) walkway – top view; (b) walkway – side view; (c) walkway – end view; (d) force plate isolation fixture diagram; (e) force plate isolation fixture model; (f) image of force plate isolation fixture in walkway.

by three variables, which were the differences in COP locations ($\Delta COPx, y, z$), the x, y and z components of the displacement vector between the COP location as determined from the force plate measurements and the tip of the MTD location as determined from the motion capture system (Fig. 2b), then averaged for the 5 trials to obtain the mean $\Delta COPx, y, z$ values at each location.

Statistical comparisons were performed using a 3 (NB, MB and WB) × 2 (level and cross-slope) repeated measures analysis of variance (ANOVA) to investigate the effect of surface condition and configuration for the $\Delta COPx, y, z$. Post hoc tests were conducted using the Bonferroni adjustment to correct for multiple comparisons. Two-sample t-test was used for exploring the possible difference between the center and corners of the force plate in both level and cross-slope conditions. Results were considered statistically significant when $p < 0.05$ ($\alpha = 0.05$). Data analyses were performed using SPSS 20.0 (IBM Corporation, Armonk, NY, USA).

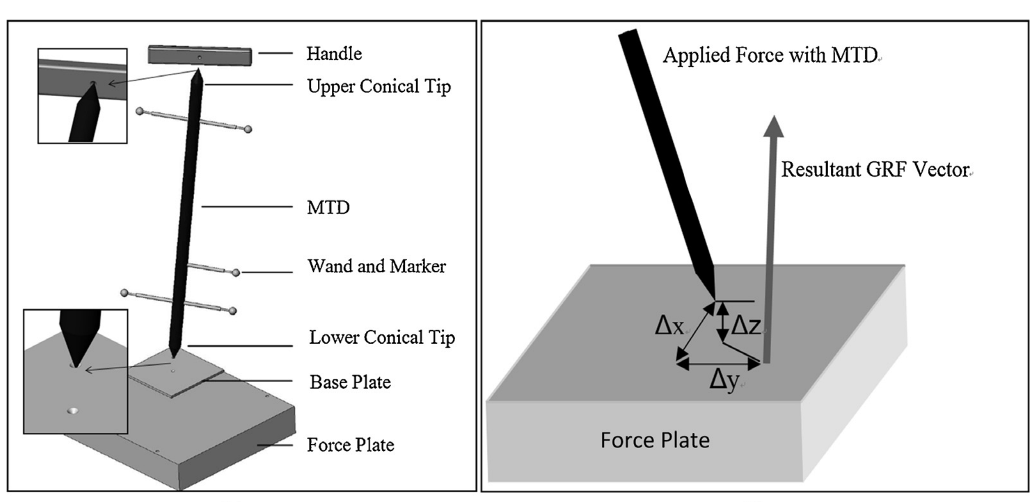

Fig. 2. Mechanical testing device (a) and the difference of COP between applied force using MTD and force plate (b).

3. Results

Ballast was initially poured directly onto the force plate with a membrane covering the force plate to prevent ballast wedging between the top plate and base plate of force platform. However, the effect was unsatisfactory and significant dispersion (up to 40% in worst case) of the measured forces occurred near the edge of the force plate when force was applied through the ballast. The effect of force dispersion is removed with the addition of the isolation fixture developed in this study.

The summary of Δ*COPx*, *y*, *z* between the calibration system and the force plate estimates is reported in Table 1. The results show that the sum of Δ*COPx*, *y*, *z* was smaller for NB than ballasts (MB and WB) in both level and cross-slope conditions. The largest Δ*COPx*, *y*, *z* (6.1 mm, 5.1 mm and 2.4 mm for Δ*COPx*, Δ*COPy* and Δ*COPz*) were all found in the WB cross-slope condition, but the sum of Δ*COPx*, *y*, *z* was quite similar between MB and WB, especially in the level condition.

A summary of results from ANOVA for Δ*COPx*, *y*, *z* (Table 2) indicated that the effects of surface condition and configuration were not statistically significantly different for Δ*COPx* ($p = 0.099$/0.791), Δ*COPy* ($p = 0.108$/0.192) and Δ*COPz* ($p = 0.160$/0.208). Post hoc tests further showed that no statistically significant differences were found among the NB, MB and WB during pairwise comparison. The Δ*COPx*, *y*, *z* between the center and corners of the force plate were compared for the level condition and cross-slope condition, respectively (Table 3). Significant differences between the center and corners of the force plate were found for Δ*COPx* ($p = 0.040$/0.013/0.001/0.014), Δ*COPy* ($p = 0.022$/0.030/0.018/0.025) and Δ*COPz* ($p = 0.003$/0.032/0.013/0.048) in ballast conditions (both MB and WB) for level and cross-slope configurations.

4. Discussion

The purpose of this study was to evaluate the feasibility of using an isolation-fixture force plate system to quantify the COPs on two types of ballasts in both level and cross-slope conditions. A calibration system was used to verify the accuracy of the results from force plate estimates. The results demonstrate that the isolation-fixture force plate system can successfully determine the COPs in ballast conditions as identified by the 3D motion tracking system. The effects of surface condition and configuration are not significant for Δ*COPx*, *y*, *z* (Table 2). No differences of Δ*COPx*, *y*, *z* among NB, MB and WB reveals that the isolation-fixture force plate system can effectively prevent the dispersion of ballast and that ballast conditions have statistically equal variances compared with the NB condition.

The average position error reported from the direct linear transformation report supplied by the Vicon motion system for the camera configuration and calibration is 0.3 ± 0.1 mm, which provides a potential explanation for the non-zero Δ*COPz* in the NB level condition. The *COPz* of ballast estimated from the force plate is only determined by the initial ballast depth above the force plate, which is a constant value (*t* in Eqs. (3) and (4)). However, the contact surface plane where the base plate for the MTD was located is not actually a constant, parallel distance above the force plate due to the ballast shape and protrusion, which is confirmed by the large Δ*COPz* in ballast conditions. This slight variation of ballast depth affects the accuracy of calculated *COPx* and *COPy* estimated by the force plate system (Eqs. (3) and (4)), which explains the finding that the magnitudes of Δ*COPx* and Δ*COPy* are found to be larger in ballast conditions than NB (Table 1). Significant differences between the center and corners of the force plate were found for Δ*COPx*, *y*, *z* in MB and WB for both level and cross-slope conditions (Table 3). A possible reason for this phenomenon is the increased shear force and ballast depth variation when applying force in the corners of the force plate due to the lack of adjoining ballast near the edge of the isolation fixture.

The COP information can be accurately measured in an environment where the force plate is used beneath the ballast to better represent environmental conditions to study human gait. This study demonstrates that isolating the force plate from the influence of the surrounding ballast provides a suitable method for recording the COP in both level and cross-slope conditions. The dissipation of force and additional error that would likely result along the edges of the force plate from a simple buried plate, as noted by others, could be reduced by incorporating an isolation fixture [19]. This benefit is expected to be observed when studying greater ballast depths and slopes as well. The treatment of ballast shown in this study may be applicable to other similar surface

Table 1
The summary of Δ*COPx*, *y*, *z* between the calibration system and the force plate estimates.

	Location	Δ*COPx* (mm)				Δ*COPy* (mm)				Δ*COPz* (mm)			
		Level		Cross-slope		Level		Cross-slope		Level		Cross-slope	
		Mean	SD	Mean	SD	Mean	SD	Mean	SD	Mean	SD	Mean	SD
NB	1	0.0	1.4	1.4	0.7	1.8	1.1	3.6	0.8	−0.4	0.2	−0.7	0.2
	2	3.0	0.8	4.2	1.3	3.0	0.8	3.4	1.7	0.1	0.1	−0.2	0.1
	3	1.3	0.8	0.1	0.9	0.8	1.5	2.7	0.8	−0.2	0.2	0.0	0.3
	4	2.7	1.2	3.4	0.6	1.2	0.7	3.6	1.2	0.4	0.2	0.5	0.4
	5	4.3	0.8	2.9	1.4	1.0	1.4	2.5	1.0	0.2	0.2	1.6	0.4
	Sum	11.3		12.0		7.8		15.8		0.1		1.2	
MB	1	3.8	2.3	3.7	1.7	3.8	1.3	4.8	1.1	0.8	1.0	1.8	0.3
	2	5.5	1.4	4.7	2.2	4.1	1.9	2.8	0.5	0.7	0.7	1.6	0.1
	3	3.0	1.1	1.4	1.6	0.6	1.4	1.9	0.9	0.3	0.3	0.3	0.4
	4	3.8	1.0	4.0	1.3	1.9	0.9	3.7	1.0	0.6	0.5	1.0	0.1
	5	4.5	0.3	2.6	1.6	1.9	2.5	4.8	1.2	0.8	0.2	0.7	0.3
	Sum	20.6		16.5		12.3		18.0		3.3		5.4	
WB	1	5.0	1.6	4.4	0.7	5.0	0.6	3.1	1.7	0.7	0.4	2.4	0.3
	2	5.0	1.4	6.1	1.7	3.2	1.6	5.0	1.1	0.8	0.3	1.2	0.4
	3	0.3	0.8	1.7	1.5	0.2	1.1	2.2	1.0	0.2	0.4	0.3	0.3
	4	4.5	2.0	3.4	1.0	2.3	1.3	5.1	0.8	1.0	0.3	0.9	0.1
	5	3.6	0.7	5.5	2.4	1.9	0.3	4.3	1.3	0.5	0.2	1.1	0.1
	Sum	18.4		21.1		12.6		19.7		3.2		5.9	

Note: A positive error represents estimates from the force plate are larger than the calibration system. Locations 1, 2, 4 and 5 are the four corners and location 3 is the center of the force plate. In the cross-slope condition, location 1 and 2 are the downslope corners and location 4 and 5 are the upslope corners of the force plate, respectively.

Table 2
Summary of results from the ANOVA and post hoc test for Δ*COPx*, *y*, *z* between the calibration system and the force plate estimates.

Parameter	*p*-Value (power)					
	Δ*COPx*		Δ*COPy*		Δ*COPz*	
Condition	0.099	(0.440)	0.108	(0.423)	0.16	(0.341)
	Bonferroni adjustment comparison					
NB – MB	0.302		0.491		0.629	
NB – WB	0.373		0.051		0.168	
MB – WB	0.998		0.997		0.999	
Configuration	0.791	(0.056)	0.192	(0.228)	0.208	(0.213)

Table 3
Summary of results for comparison Δ*COPx*, *y*, *z* between the center and corners of the force plate estimates.

Center vs. corners		*p*-Value		
		Δ*COPx*	Δ*COPy*	Δ*COPz*
Level	NB	0.276	0.116	0.353
	MB	0.040*	0.022*	0.003*
	WB	0.001*	0.018*	0.013*
Cross-slope	NB	0.125	0.059	0.595
	MB	0.013*	0.030*	0.032*
	WB	0.014*	0.025*	0.048*

* Significant difference at $\alpha = 0.05$.

conditions, such as sand, however, additional displacement tracking for the depth above the force plate would be required for improving the accuracy in measured COP [25].

Some limitations of this study should be mentioned. When studying a surface media subject to shifting and deformation, it may be important to study the surface in a more natural environment to capture pure, unrestricted motion. The current isolation fixture somewhat constrains the ballast movement in a compacted enclosure and may limit horizontal ballast displacements to cause shear force against the fixture. Therefore, this system most closely represents compacted ballast. A more complex method may be needed when conducting a study where significant displacements occur in the surface plane during loading on the force plate (such as the case with loose sand). In addition, although acceptable estimations for the COP values using the force plate system were verified for five locations, the accuracy to estimate the COPs during a dynamic situation, such as walking was not directly studied. Future studies focused on the dynamic evaluation of this system would be beneficial to extend the current findings.

In conclusion, the isolation fixture technique proposed in the present study demonstrates the feasibility of accurately measuring the COP using force plates for biomechanics studies on ballast surfaces that are level or cross-slope, though some potential limitations do exist. This system is expected to expand the scope of biomechanical analysis and improve our understanding of injury development when walking on ballast.

Acknowledgements

This work was supported by University Science Research Project of Jiangsu Province (14KJB310022), Scientific Research Foundation for Excellent Talents of Xuzhou Medical College (D2014018). This work was also supported, in part, by the Rocky Mountain Center for Occupational and Environmental Health NIOSH Education and Research Center training grant T42/CCT810426-10 at the University of Utah.

Conflict of interest statement

The authors attest that there are no conflicts of interest to disclose.

References

[1] Dierick F, Penta M, Renaut D, Detrembleur C. A force measuring treadmill in clinical gait analysis. Gait Posture 2004;20:299–303.
[2] Herzog W, Nigg BM, Read LJ, Olsson E. Asymmetries in ground reaction force patterns in normal human gait. Med. Sci. Sports Exerc. 1989;21:110–4.
[3] Watt JR, Franz JR, Jackson K, Dicharry J, Riley PO, Kerrigan DC. A three-dimensional kinematic and kinetic comparison of overground and treadmill walking in healthy elderly subjects. Clin. Biomech. 2010;25:444–9.
[4] Dixon PC, Böhm H, Döderlein L. Ankle and midfoot kinetics during normal gait: a multi-segment approach. J. Biomech. 2012;45:1011–6.
[5] Lejeune TM, Willems PA, Heglund NC. Mechanics and energetics of human locomotion on sand. J. Exp. Biol. 1998;201:2071–80.
[6] Zamparo P, Perini R, Orizio C, Sacher M, Ferretti G. The energy cost of walking or running on sand. Eur. J. Appl. Physiol. 1992;65:183–7.
[7] Pinnington HC, Lloyd DG, Besier TF, Dawson B. Kinematic and electromyography analysis of submaximal differences running on a firm surface compared with soft, dry sand. Eur. J. Appl. Physiol. 2005;94:242–53.
[8] Allet L, Armand S, de Bie RA, Pataky Z, Aminian K, Herrmann FR, et al. Gait alterations of diabetic patients while walking on different surfaces. Gait Posture 2009;29:488–93.
[9] Menz HB, Lord SR, Fitzpatrick RC. Acceleration patterns of the head and pelvis when walking on level and irregular surfaces. Gait Posture 2003;18:35–46.
[10] Andres RO, Holt KG, Kubo M. Impact of railroad ballast type on frontal plane ankle kinematics during walking. Appl. Ergon. 2005;36:529–34.
[11] Wade C, Redfern MS, Andres RO, Breloff SP. Joint kinetics and muscle activity while walking on ballast. Hum. Factors 2010;52:560–73.
[12] Schwameder H, Lindenhofer E, Müller E. Walking: effect of walking speed on lower extremity joint loading in graded ramp walking. Sports Biomech. 2005;4:227–43.
[13] Kang J, Chaloupka EC, Mastrangelo AM, Hoffman JR. Physiological and biomechanical analysis of treadmill walking up various gradients in men and women. Eur. J. Appl. Physiol. 2002;86:503–8.
[14] Lay AN, Hass CJ, Richard Nichols T, Gregor RJ. The effects of sloped surfaces on locomotion: an electromyographic analysis. J. Biomech. 2007;40:1276–85.
[15] Dixon PC, Pearsall DJ. Gait dynamics on a cross-slope walking surface. J. Appl. Biomech. 2010;26:17–25.
[16] Damavandi M, Dixon PC, Pearsall DJ. Ground reaction force adaptations during cross-slope walking and running. Hum. Mov. Sci. 2012;31:182–9.
[17] Damavandi M, Dixon PC, Pearsall DJ. Kinematic adaptations of the hindfoot, forefoot, and hallux during cross-slope walking. Gait Posture 2010;32:411–5.
[18] Merryweather A, Yoo B, Bloswick D. Gait characteristics associated with trip-induced falls on level and sloped irregular surfaces. Minerals 2011;1:109–21.
[19] Wade C, Redfern MS. Ground reaction forces during human locomotion on railroad ballast. J. Appl. Biomech. 2007;23:322–9.
[20] Bonnett CF. Practical Railway Engineering. Imperial College Press; 2005.
[21] Holden JP, Selbie WS, Stanhope SJ. A proposed test to support the clinical movement analysis laboratory accreditation process. Gait Posture 2003;17: 205–13.
[22] Rabuffetti M, Ferrarin M, Benvenuti F. Spot check of the calibrated force platform location. Med. Biol. Eng. Comput. 2001;39:638–43.
[23] Kiss RM. Comparison between kinematic and ground reaction force techniques for determining gait events during treadmill walking at different walking speeds. Med. Eng. Phys. 2010;32:662–7.
[24] Sinclair J, Hobbs SJ, Protheroe L, Edmundson CJ, Greenhalgh A. Determination of gait events using an externally mounted shank accelerometer. J. Appl. Biomech. 2013;29:118–22.
[25] Xu H, Wang Y, Greenland K, Bloswick D, Merryweather A. The influence of deformation height on estimating the center of pressure during level and cross-slope walking on sand. Gait Posture 2015;42:110–5.